ingegneria sismica
International Journal of Earthquake Engineering
Anno XLIII - Num. 1 - 2026

Research on Intelligent Construction and Management Model Innovation of Underground Pipeline Tunnels Driven by Urban Information Model in the Context of Smart City Update

Xuehao Chen[1] *and Ruiming Lan*[2,*]

[1] Sichuan Technology and Business University,Chengdu 611745, Sichuan, China
[2] Southwest Jiaotong University Hope College,Chengdu 610400, Sichuan, China

SUMMARY: *In the context of smart city renewal, there are issues such as data fragmentation and disconnection in underground integrated pipe galleries. This paper takes the urban information model as the core: (1) It constructs a three-layer CIM data model at the city level, engineering level, and asset level, and proposes a multi-source data integration algorithm of "spatial-semantic-time alignment + integrity evaluation"; (2) Oriented towards the number of collisions, rework costs, and operation-friendliness, it designs a multi-objective optimization and 4D construction rolling scheduling algorithm, and automatically re-arranges the plan when the deviation of key tasks exceeds 1 day or 5%; (3) It introduces equipment health index HI and environmental risk index R, and builds a "monitoring - prediction - work order" intelligent operation and maintenance algorithm chain. Engineering applications show that the data integrity during the construction stage has increased from 0.62 to 0.88, and the progress fulfillment has increased from 0.70 to 0.86. During the operation and maintenance stage, the inspection coverage rate has increased from 0.68 to 0.90, and the annual failure rate has decreased from 0.42 to 0.21 times/unit/year, verifying the effective support of the CIM-driven algorithm system for the intelligent construction and operation of underground pipe galleries.*
Povzetek: Using City Information Modelling (CIM), this paper builds a three-layer city–project–asset data model with algorithms for data integration, design optimization, rolling construction scheduling and predictive O&M, unifying surveying, design, construction and operation data in a single object library.

KEYWORDS: *CIM; Underground Integrated Utility Tunnel; Multi-source Data Integration; Collaborative Design Optimization*

1 Introduction

The underground integrated pipe gallery, as a key infrastructure that carries multiple professional pipelines such as water supply, electricity, communication, and gas, its structural safety, environmental control, and operation maintenance level directly affect the resilience of the urban lifeline projects. Regarding the structural performance, Enhua Zhang et al. conducted full-scale tests on prefabricated pipe galleries using flexible energy dissipation nodes, systematically revealing the force responses and energy dissipation characteristics under different node configurations, providing experimental basis for seismic and ductility design [1]; Xintao Yu et al. and Deng Botuan et al. started from the conditions of ground fissures displacement and surface fissure development, calculated the range of bottom cavities and

*cimstudio@163.com
https://doi.org/10.65102/is2026023
Published: 30 April, 2026

analyzed the internal forces and deformation patterns of the pipe gallery structure under the action of fissures [5, 10]; Xie Junfei et al. conducted research on the deformation laws of shallow-buried underground pipe galleries, pointing out the influence of soil cover conditions, adjacent structures, and load conditions on the safety reserve of the structure [11]. Beyond the structure, some works further focused on the coupling utilization of pipe galleries with buildings-environment systems, for example, Tong Wei et al. coupled the pre-cooling of underground pipe galleries with post-heating by PV/T after heating in the built-in chimney ventilation system, quantifying the synergistic effect of pre-cooling and post-heating on ventilation and energy-saving performance [2], and in another experimental study, investigated the impact of the combined scheme of "pipe gallery ventilation + underground heat exchange" on cooling performance [6], indicating that the rational utilization of pipe gallery space and temperature fields is expected to significantly improve the energy performance of buildings and urban micro-environments.

In terms of safety and environmental management, Soukaina Bakkass et al. took a certain underground corridor project in Casablanca as an example, introducing the ISO 14001 environmental management system to the construction site of the pipe gallery, proving that standardized environmental management can reduce construction disturbance and environmental risks [3]; Moussa Diallo et al. conducted interviews with stakeholders of the underground mine tunnel collapse in Guinea to reveal the hazards of insufficient risk perception and regulatory deficiencies in underground space operations [7]; Dorthi Kumar and Karra Ram Chandar proposed an integrated IoT slope monitoring system for long-term monitoring and early warning of the overburden slope stability of old underground tunnels [9]. At the operation and maintenance level, Haoyue Lin et al. proposed a UWB adaptive fusion-based pipeline gallery inspection positioning method, improving the positioning accuracy of mobile terminals in irregular environments [4]; Gaifang Xin et al. used WSNs distributed perception to explore the path perception and data collection problems of mobile robots in irregularly structured pipe galleries [8]; Sungyeol Lee et al. constructed an AI damage risk prediction model based on pipeline attribute information for the active operation and maintenance of thermal pipelines, providing ideas for the active operation and maintenance of thermal networks [14]. These studies collectively indicate that through multi-source sensing, IoT, and intelligent algorithms, the monitoring accuracy and early warning capability of underground corridors can be significantly improved, but they mainly focus on local optimization at the level of a single project or system.

At the same time, the information modeling and spatial decision-making technologies at the urban scale are developing rapidly. Bin Sun proposed a theoretical model and prediction framework for the rapid evolution of urban building fires based on GIS, demonstrating the possibility of rapid simulation of urban-scale fire scenarios [12]; Yulia Karpova et al. constructed a multi-objective optimization model and implemented urban green space site selection using GIS tools [15]; Maosu Li et al. proposed an efficient evaluation method for the distance to the window landscape using urban information models and 3D computer vision technology [16]. In the field of urban information model ontology, Luqi Wang et al. systematically reviewed the research context and hot topics of CIM supporting sustainable smart city governance from the perspective of bibliometric analysis [13]. Na Luo et al. proposed a data exchange mode for coupling simulation of urban building energy consumption model and urban microclimate model [17]; Zijian Xu et al. utilized the geometric prior of the visual basic model to enhance the automatic mapping of urban open spaces [18]; Anran Li et al. fused the cellular transmission model with Transformer to construct a spatio-temporal graph model of urban signal intersection traffic state [19]; Ahmad Askari Lasaki et al. introduced soft

computing and intuitive fuzzy information to depict the interdependence of indicators in the evaluation of urban concrete bridge maintenance models [20]. These studies focusing on fields such as buildings, transportation, and green spaces indicate that multi-source data modeling and intelligent decision-making technologies centered on CIM/GIS have become important supporting tools for smart city governance.

In summary, current research on underground pipe galleries has achieved rich results in aspects such as structural response, ventilation energy efficiency, and construction environment management, and also shows certain potential in monitoring perception and local intelligent operation and maintenance. However, most of it remains at the level of individual projects or local systems; at the same time, research on CIM and intelligent algorithms at the urban scale has advanced, but it rarely integrates underground comprehensive pipe galleries as the "urban lifeline" into the urban-level information model framework. Especially in the context of smart city renewal, how to construct an integrated data and algorithm system of "urban information model - underground pipe gallery project - intelligent operation and maintenance" at the urban scale, connect the full cycle data chain from surveying to design, construction, and operation and maintenance, and through scheduling optimization, status assessment, and risk prediction algorithms to form a quantifiable and reusable intelligent management model, still lacks systematic research. Based on this, this paper builds a city information model-driven intelligent construction and management model for underground pipe galleries from three levels: multi-source data integration, intelligent construction scheduling, and intelligent operation and maintenance evaluation, aiming to achieve integrated intelligent management of the entire life cycle of pipe galleries in urban renewal scenarios.

2 Related Works

2.1 The three-layer data model of the underground pipe gallery CIM and the multi-source data integration technology during the construction stage

To support the precise management of the entire process of the underground pipe gallery from the design phase to the construction implementation, this study has constructed a three-layer CIM data model consisting of the city level, engineering level and asset level, and proposed an integrated technology for multi-source data in the construction stage, including surveying, design and construction. The three layers maintain strict temporal and spatial constraints and encoding mapping relationships, providing a unified data foundation for subsequent collaborative design, four-dimensional construction and operation monitoring.

From a formal perspective, the three-layer object sets are respectively represented as:

$$L^{city},\ L^{proj},\ L^{asset} \tag{1}$$

Among them, L^{city} is the city-level spatial object set (road red line, terrain, existing buildings and existing pipelines, etc.), L^{proj} is the underground pipe gallery engineering-level object set (pipe gallery sections, compartments, node structures, etc.), and L^{asset} is the asset-level object set (electrical and mechanical equipment, ancillary components, sensors, etc.). The three sets satisfy nested constraints:

$$L^{asset} \subset L^{proj} \subset L^{city} \tag{2}$$

Formula (2) constrains that asset objects must be attached to specific engineering objects,

and engineering objects must be embedded in the urban spatial framework, thus ensuring that all construction stage data can be located within the unified urban temporal and spatial system.

The multi-source data in the construction stage can be abstracted as a data source set:

$$\mathcal{D} = \mathrm{D}^{\mathrm{surv}} \cup \mathrm{D}^{\mathrm{des}} \cup \mathrm{D}^{\mathrm{const}} \tag{3}$$

Among them, $\mathrm{D}^{\mathrm{surv}}$ is the surveying and existing pipeline detection data, $\mathrm{D}^{\mathrm{des}}$ is the two-dimensional/three-dimensional design data and calculation results, and $\mathrm{D}^{\mathrm{const}}$ is the process data of construction stage progress, quality, safety and change visa. The core issue of data integration is to construct a unified mapping function from raw data to CIM objects:

$$\mathrm{f}: \mathcal{D} \rightarrow \mathrm{L}^{\mathrm{city}} \cup \mathrm{L}^{\mathrm{proj}} \cup \mathrm{L}^{\mathrm{asset}} \tag{4}$$

that projects different sources and formats of data to corresponding levels of CIM objects and their attributes.

To build a computable mapping relationship, this study adopts a three-step integration strategy of "spatial alignment + semantic alignment + time alignment":

(1) Spatial alignment. Firstly, unify the survey data, design coordinate system and construction measurement coordinate system, and align different data sources to the unified city coordinate system CScity using rigid body transformation. Let the original coordinates be: $\mathrm{x_i}$, and the aligned coordinates be $\mathrm{x'_i}$, then:

$$x'_i = R\,x_i + t \tag{5}$$

Among them, R is the three-dimensional rotation matrix, and t is the translation vector. By minimizing the registration error:

$$\min_{\mathrm{R,t}} \sum_{\mathrm{i=1}}^{\mathrm{n}} \left\| \mathrm{x'_i} - \mathrm{x_i^{ref}} \right\|^2 \tag{6}$$

achieve the unification of survey control points, design reference points and construction measurement points, so that subsequent data can be attached to $\mathrm{L}^{\mathrm{city}}$ or $\mathrm{L}^{\mathrm{proj}}$ objects in the same spatial framework.

(2) Semantic alignment. For the problem of inconsistent field names and different granularities of data in different stages, construct a unified attribute dictionary A, define attribute names, data types and units, and establish mapping tables ϕ for the fields in survey results, design results and construction records. Map the original field αkraw to the standard field αkstd:

$$\phi: \alpha_{\mathrm{k}}^{\mathrm{raw}} \mapsto \alpha_{\mathrm{k}}^{\mathrm{std}} \in \mathcal{A} \tag{7}$$

For example, unify "pavement number", "mileage" and "K value" as "Chainage", and unify "plate thickness" and "thickness" as "Thickness". On this basis, construct object–attribute pairs $(o_j, \{\alpha_{j,m}^{std}\})$, and load the data into the corresponding $\mathrm{L}^{\mathrm{city}}$, $\mathrm{L}^{\mathrm{proj}}$ or $\mathrm{L}^{\mathrm{asset}}$ objects.

(3) Time alignment. For process data such as construction progress, quality inspection, concealed acceptance and change visa, use a unified time stamp t to record it, and establish a time series relationship with the object set. The state sequence of a component object oj during the construction phase can be expressed as:

$$S(o_j) = \{(t_1, s_1), (t_2, s_2), \dots, (t_K, s_K)\} \quad (8)$$

Among them, s_K represents the state label at that moment, such as "not constructed", "under construction", "awaiting acceptance", "accepted", "rectified", etc. This time series can be used for both four-dimensional construction simulation and subsequent quality traceability and operation maintenance preparation.

To evaluate the data integration quality during the construction phase, this study introduces an object-level data integrity indicator. Let M_j^{target} be the number of target attributes corresponding to object oj, and M_j^{filled} be the actual filled attributes. Then, the integrity of object o_j is:

$$Comp(o_j) = \frac{M_j^{filled}}{M_j^{target}} \quad (9)$$

The average integrity of the entire engineering asset layer can be expressed as:

$$\overline{Comp} = \frac{1}{N}\sum_{j=1}^{N} Comp\,(o_j) \quad (10)$$

Among them, N is the total number of asset objects. Through continuous monitoring of Comp, weak links in data integration can be identified, and key attribute fields can be promptly supplemented and corrected to ensure that the delivered model is operable.

According to the above definition, the implementation process of multi-source data integration technology during the construction stage can be summarized as follows (as shown in Figure 1): data source organization and field standardization → coordinate unification and spatial alignment → attribute mapping and object connection → status annotation and time alignment → overall consistency and integrity check. Specifically, in the "data source organization and field standardization" stage, heterogeneous data such as surveying, design, construction logs, quality inspection, BIM/CAD models, etc. are classified and sorted, and similar information is unified under a consistent field naming and coding system; then through "coordinate unification and spatial alignment", the planar coordinates and elevation systems from different sources are converted to a unified CIM urban coordinate system, and feature points, control points, and component outlines are used for spatial precise alignment; on this basis, "attribute mapping and object connection" is executed, where component numbers, segment information, professional attributes, etc. are mapped to the CIM object library to achieve one-to-one correspondence between "data record - spatial object - engineering component"; then "status annotation and time alignment" is completed, adding information such as construction stage, task status, inspection results, timestamp, etc. to each record to support subsequent query and analysis along the time axis; finally, through "overall consistency and integrity check", automatic verification of indicators such as coordinate closure, coding uniqueness, and missing rate of required fields is conducted, and quantifiable integrity evaluation results are output.

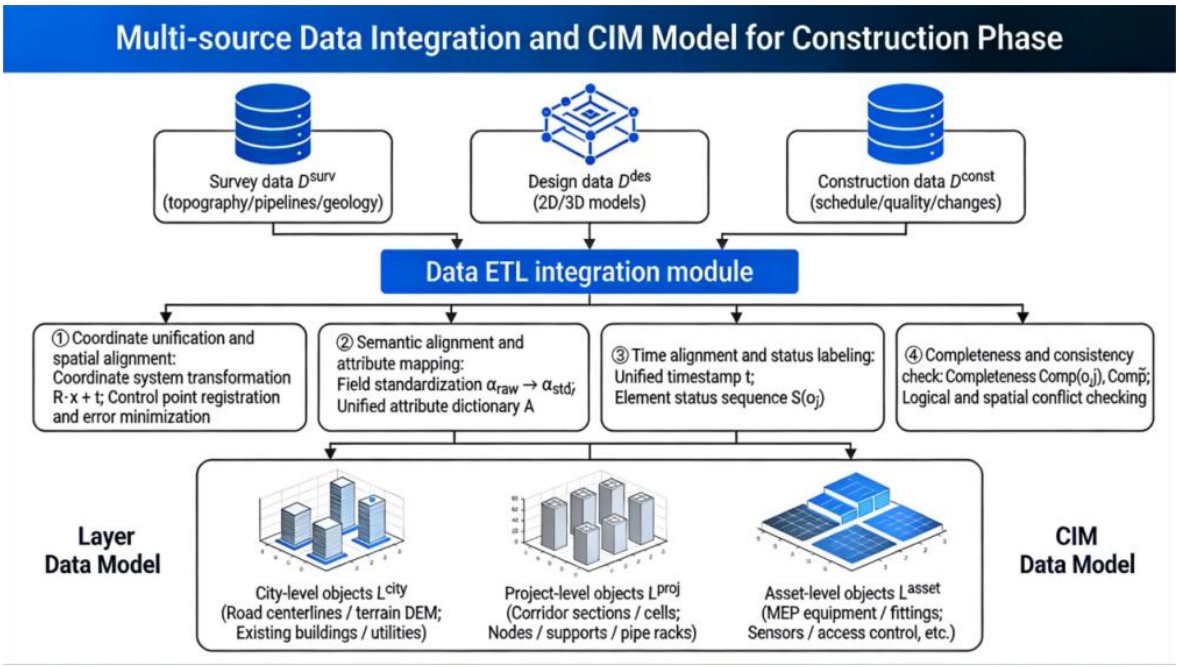

Figure 1: Schematic diagram of the three-layer CIM data model for underground pipe galleries and the integration relationship of multi-source data during the construction stage.

Figure 1 illustrates the relationship between the multi-source data integration during the construction phase and the three-layer CIM data model of the underground pipe gallery. From top to bottom, there are three types of data sources: survey data Dsurv (terrain, pipelines, geology, etc.), design data Ddes (two-dimensional/three-dimensional models), and construction data Dconst (progress, quality, change records). These data first enter the Data ETL integration module in the middle, where four steps are sequentially completed within this module: (1) Coordinate unification and spatial alignment, including coordinate system transformation R_{x+t} and control point registration and error minimization; (2) Semantic alignment and attribute mapping, achieving consistency of different data source fields through field standardization αraw→αstd and unified attribute dictionary A; (3) Time alignment and status annotation, constructing a component status sequence $S(o_j)$ through a unified timestamp t ; (4) Completeness and consistency check, calculating object completeness indicators $Comp(o_j)$ and $\overline{\text{Comp}}$, and conducting logical and spatial conflict verification. Below is the three-layer CIM data model object library, including city-level objects L_{city} (road centerlines, terrain DEM, existing buildings and municipal pipelines), engineering-level objects L_{proj} (segmentation of the pipe gallery, compartments, nodes, supports and pipe racks), and asset-level objects L_{asset} (electrical and mechanical equipment, ancillary components, sensors and access control, etc.). Through this data pipeline, the multi-source heterogeneous data during the construction phase is standardized and processed and then written into the three-layer CIM object library, providing integrated data support for the intelligent construction and intelligent operation and maintenance of the underground pipe gallery in the future.

2.2 Collaborative Design Based on CIM: Four-Dimensional Construction and Operation Monitoring, Integrated Predictive Maintenance Management Method

Based on the three-layer CIM data model and multi-source data integration established, this section presents a set of integrated management methods that cover collaborative design, four-

dimensional construction, operation monitoring, and predictive maintenance, enabling the underground pipe gallery to operate in a closed loop within the same model and data system from design to operation.

During the collaborative design stage, multiple professional models such as structures, buildings, pipelines, and electromechanical systems are uniformly loaded into the CIM platform to form a model collection:

$$\mathrm{M} = \{\mathrm{M}^{\mathrm{str}}, \mathrm{M}^{\mathrm{arch}}, \mathrm{M}^{\mathrm{pip}}, \mathrm{M}^{\mathrm{mep}}, \ldots\} \tag{11}$$

The design variables such as the elevation of the corridor, the cross-sectional dimensions, and the pipeline markers are represented by the adjustable parameter vector x. The scheme is quantitatively evaluated through the collision quantity $C(x)$, the rework risk cost $R(x)$, and the operation and maintenance friendliness $E(x)$, and a multi-objective design optimization model is constructed as follows:

$$\min_{\mathrm{x}} \mathrm{F}(\mathrm{x}) = \mathrm{w}_1\mathrm{C}(\mathrm{x}) + \mathrm{w}_2\mathrm{R}(\mathrm{x}) - \mathrm{w}_3\mathrm{E}(\mathrm{x}) \tag{12}$$

Among them, w_1, w_2, w_3 are the weight coefficients. Each scheme iteration $x(k)$ corresponds to a version v in CIM, and the differences between versions can be expressed as:

$$\Delta\mathrm{M}^{(\mathrm{k})} = \mathrm{M}(\mathrm{x}^{(\mathrm{k})}) - \mathrm{M}(\mathrm{x}^{(\mathrm{k}-1)}) \tag{13}$$

The platform records the objects and attributes involved in $\Delta M^{(k)}$, achieving precise tracking of multi-disciplinary changes. The overall process of collaborative design is shown in Figure 2.

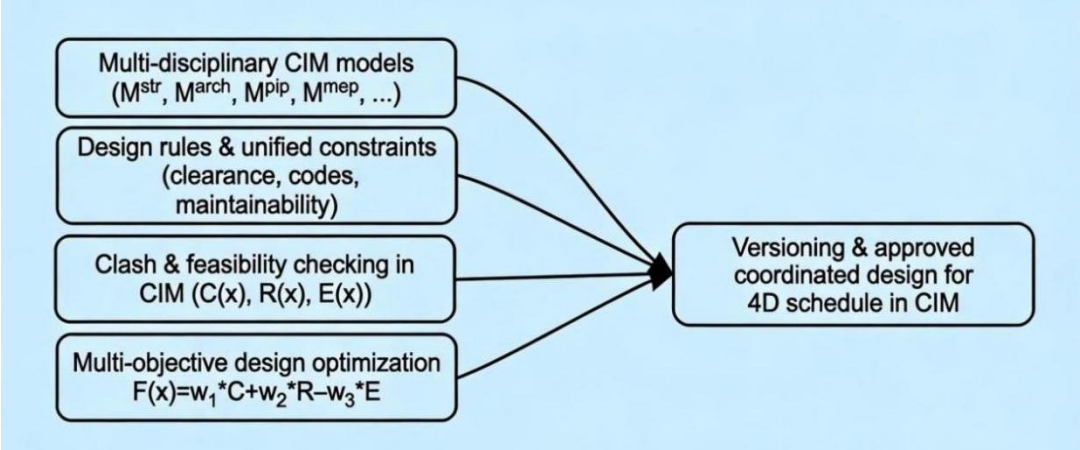

Figure 2: Schematic diagram of the collaborative design workflow based on CIM.

To facilitate engineering implementation, the collaborative design process is abstracted into the following multi-objective optimization algorithm.

Steps of the collaborative design multi-objective optimization algorithm:

1. Initialize the design parameter vector $x(0)$, load the initial models of each specialty Mstr, March, Mpip, Mmep.

2. Generate version v0 in CIM, perform collision detection and accessibility check, calculate $C(x(0))$, $R(x(0))$, $E(x(0))$, and obtain $F(x(0))$.

3. According to the design rules and constraints, generate a candidate solution set $\{x_1^{(k)}, \ldots, x_q^{(k)}\}$ from $x^{(k)}$ (such as adjusting the height of the corridor, local section form,

pipeline marking, etc.).

4. Update the CIM model for each candidate solution $x_j^{(k)}$, perform collision detection and operation accessibility analysis, and calculate $F(x_j^{(k)})$.

5. Select the optimal solution $x^{(k+1)}$ according to the weighted sum minimum or Pareto sorting in CIM, form a new version v^{k+1}, and record $\Delta M^{(k+1)}$.

6. If $| F(x^{(k+1)}) - F(x^{(k)}) | < \varepsilon$ or the number of iterations reaches the upper limit, stop the iteration and output the final solution x^*; otherwise, set $k \leftarrow k + 1$ and return to step 3.

The corresponding pseudo-code can be organized as follows. Algorithm 1 CIM-based multi-objective collaborative design

Input:
Initial design x(0)
Multi-discipline models M
Weights w_1, w_2, w_3
Tolerance ε Maximum iterations maxIter
Output:
Optimized design x^*
1:k ← 0
2:Build CIM version v0 with x(0)
3:Run clash and maintainability checks on v0
4:Compute $C(x(0))$, $R(x(0))$, $E(x(0))$
5:F(x(0)) ← w1*C(x(0)) + w2*R(x(0)) − w3*E(x(0))
6:while k < maxIter do
7:Generate candidate set { x_{k^1}, ... , x_{k^q}} from $x^{(k)}$
8:for each candidate x_k^j in { $x_1^{(k)}$, … , $x_q^{(k)}$} do
9:Update CIM model with $x_j^{(k)}$
10:Run clash and maintainability checks
11:Compute $F(x_j^{(k)})$.
12:end for
13:$x^{(k+1)} \leftarrow argmin_j Fx_j^{(k)}$
14: Record the model difference $\Delta M^{(k+1)}$ between versions v^k and v^{k+1}
15: if $| F(x^{(k+1)}) - F(x^{(k)}) | < \varepsilon$ then 16:$x* \leftarrow x^{(k+1)}$
17:break
18:end if
19:$k \leftarrow k + 1$
20:end while
21:return $x*$

During the four-dimensional construction phase, the construction tasks are represented as:

$$T = \{\tau_1, \tau_2, \ldots, \tau_n\} \tag{14}$$

Each task τ_i is associated with a set of CIM objects $\Omega(\tau_i) \subseteq L_{proj} \cup L_{asset}$, and has a planned start time s_i and completion time f_i. The four-dimensional construction mapping can be written as:

$$g: T \rightarrow (\Omega(\tau_i), s_i, f_i) \tag{15}$$

Under the premise of satisfying process logic, resource capacity and space occupation

constraints, with the goal of the shortest total construction period:

$$\begin{aligned} \min \quad & \max_i f_i \\ \text{s.t.} \quad & s_j \geq f_i, \quad \forall (\tau_i \prec \tau_j) \\ & \sum_{\tau_i \in T_r(t)} r_i \leq R^{max}, \quad \forall t \\ & \Phi(\Omega(\tau_i), \Omega(\tau_j), t) \leq 0 \end{aligned} \tag{16}$$

Among them, $\tau_i \prec \tau_j$ represents the sequence relationship of processes, r_i is the resource requirement of the task, R_{max} is the resource upper limit, and $\Phi(\cdot)$ is the spatial conflict criterion. At any time t, the current set of objects in the construction state $\Xi(t)$ can be obtained through:

$$\Xi(t) = \{ o_j \parallel \exists \tau_i, o_j \in \Omega(\tau_i), s_i \leq t \leq f_i \} \tag{17}$$

This enables the visualization replay of the construction scenario and the analysis of the construction window. The corresponding four-dimensional construction scheduling can be expressed in the following pseudo-code.

Algorithm 2 4D schedule optimization under CIM constraints

Input:

Task set T

Precedence relations ($\tau_i \prec \tau_j$) Resource limit R^max

Space conflict function $\Phi(\cdot)$ Maximum iterations max Iter

Output:

A feasible schedule { s_i, f_i } for all $\tau_i \in T_1$:Initialize schedule { s_i, f_i } using critical path method

2:iter ← 0

3:repeat

4:feasible ← true

5:for each time slice t in planning horizon do

6:Compute active task set $T_r(t)$

7: If the sum of r_i over all τ_i belonging to $T_r(t)$ is greater than R^max, then 8:feasible ← false

9:Adjust start times of some tasks in $T_r(t)$

10:end if

11: Check $\Phi(\Omega(\tau_i), \Omega(\tau_j), t)$ for all task pairs (τ_i, τ_j) in $T_r(t)$

12: If any $\Phi(\Omega(\tau_i), \Omega(\tau_j), t)$ is greater than 0 then 13:feasible ← false

14:Adjust start times of conflicting tasks

15:end if

16:end for

17:iter ← iter + 1

18:until feasible = true or iter ≥ maxIter

19:return { s_i, f_i }

Entering the operation stage, the monitoring indicators of each device $e_k \in L_{asset}$ are combined into a vector:

$$z_k(t) = [z_{k1}(t), z_{k2}(t), \ldots, z_{km}(t) \tag{18}$$

After normalization, $z'_{kp}(t) \in [0,1]$ is obtained, and the equipment health index is

constructed:

$$\mathrm{HI_k(t)} = \sum_{\mathrm{p=1}}^{\mathrm{m}} \omega_{\mathrm{p}}\ \mathrm{z'_{kp}(t)}, \quad 0 \le \mathrm{HI_k(t)} \le 1, \sum_{\mathrm{p=1}}^{\mathrm{m}} \omega_{\mathrm{p}} = 1 \tag{19}$$

When $HI_k(t)$ is lower than the alarm threshold θ_{warn} or the critical threshold θ_{crit}, it is respectively determined as a warning state and a serious state. For the environmental monitoring data of the cabin or section, the vector $y_s(t)$ (temperature, humidity, gas concentration, water accumulation level, etc.) is formed, and the risk index is defined:

$$\mathrm{y_s(t)} = [\,\mathrm{y_{s1}(t)}, \mathrm{y_{s2}(t)}, \ldots, \mathrm{y_{sq}(t)}\,] \tag{20}$$

Among them, λ_{sq} is the allowable value of each indicator. When $R_s(t) > 1$, partition s is determined as an environmental high-risk area and highlighted in the CIM model.

In the predictive maintenance stage, based on the HI curve and historical fault records, the remaining life of key equipment is estimated. Assuming that the health index degrades approximately linearly over time:

$$\mathrm{R_s(t)} = \max_{\mathrm{q}} \left(\frac{\mathrm{y_{sq}(t)}}{\lambda_{\mathrm{sq}}} \right) \tag{21}$$

Then the predicted time to reach the critical threshold θ_{crit} is:

$$\mathrm{t_f} = \frac{\theta_{\mathrm{crit}} - \mathrm{a_k}}{\mathrm{b_k}} \tag{22}$$

When $t_f - t_0 < \Delta \mathrm{T_{maint}}$ (t_0 is the current time, $\Delta \mathrm{T_{maint}}$ is the maintenance lead time), the system will include device $\mathrm{e_k}$ in the predictive maintenance list and generate a preventive work order. According to the health status and environmental risk, the maintenance strategy function:

$$\pi\colon (\mathrm{HI_k(t)}, \mathrm{R_s(t)}) \rightarrow \mathrm{a_k} \in \{\mathrm{inspect, repair, replace}\} \tag{23}$$

Provides action decisions such as "inspection/repair/replacement". The overall operation monitoring - predictive maintenance - work order closed-loop logic is shown in Figure 3.

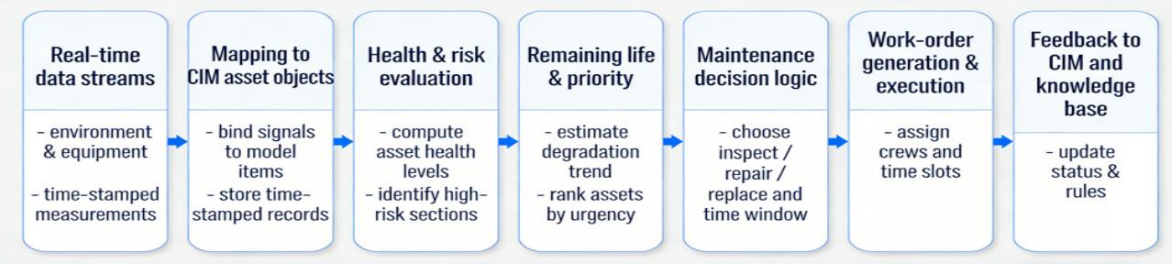

Figure 3: Monitoring - Predictive Maintenance - Work Order Closed-loop Management Illustration.

The corresponding monitoring - prediction - work order closed-loop can be abstracted into the following algorithm. Algorithm 3 Monitoring–prediction–work-order loop

Input:

Real-time streams $z_k(t)$, $y_s(t)$
Warning threshold θ_{warn}
Critical threshold θ_{crit}
Maintenance lead time ΔT_{maint} Output:
Work-order list
Updated $HI_k(t)$ for all assets
1:for each time step t do
2:for each asset e_k do
3:Compute normalized indicators $z'_k(t)$ from $z_k(t)$
4: $HI_k(t) \leftarrow \Sigma_p\ \omega_p \cdot z'_{kp}(t)$
5:end for
6:for each section s do
7: Compute $R_s(t)$ using $y_s(t)$ and the limits λ_{sq}
8:end for
9:for each asset e_k do
10:Fit degradation model $HI_k(t) \approx a_k + b_k(t)$
11: $t_f \leftarrow (\theta_{crit} - a_k) / b_k$
12: if $HI_k(t) < \theta_{crit}$ or $(t_{f-t}) < \Delta T_{maint}$ then 13:action ← "preventive repair"
14: else if $HI_k(t) < \theta_{warn}$ then 15:action ← "inspection"
16:else
17:action ← "none"
18:end if
19:if action ≠ "none" then
20:Create work order w_1 for asset e_k with action
21:end if
22:end for
23:end for

Through the aforementioned collaborative design, four-dimensional construction, and operation monitoring - predictive maintenance algorithms and processes, the CIM model is continuously data-driven and updated from the design stage to the construction and operation stages, achieving integrated management of collaborative design, construction scheduling, and operation decision-making, and providing unified technical support for the intelligent construction and management of underground pipe galleries in the context of smart city renewal.

3 Results

3.1 Application Effect and Performance Verification of the Intelligent Construction Model for Underground Pipe Lanes Driven by Urban Information Model

In the same underground pipeline corridor section, a baseline group (using a conventional management method of two-dimensional drawings and manual ledgers) and an experimental group (CIM-driven, using the city information model as the data foundation, combined with ETL data alignment, 4D rolling scheduling, and quality and safety closed-loop management) are set up.Under the unified weekly statistical framework.The progress deviation, defect density, closed-loop duration, and key performance indicators are compared and evaluated. All data are automatically generated by "Object Status Record - Scheduling Log - Work Order Log", avoiding subjective errors and inconsistent measurement standards caused by manual statistics.

The experimental running environment and key parameter settings are shown in Table 1: The system realizes data refresh once a day through the ETL process, unifying coordinates, fields, and timestamps for multi-source data from surveying, design, construction, and operation and maintenance; generating weekly plans with a 7-day rolling window, binding tasks with objects such as components, segments, and equipment to form a traceable task-object mapping; when the planned-actual deviation of key tasks exceeds 1 day or 5%, the rolling scheduling algorithm is automatically triggered to locally rearrange critical paths and high-conflict tasks, and synchronously write back to the CIM model and on-site briefing list; for the quality and safety side, all defects and hazards are recorded and bound to object IDs and segments, clustering and identifying high-frequency problem areas based on features such as "segment, defect type, process, and severity", generating a list of key inspection points, and promoting timely closed-loop through five-state work orders (discovery, assignment, rectification, re-inspection, closure), upgrading automatically when overdue, forming a risk convergence process.

Table 1: Experimental Environment and Key Parameters.

Item	Values/Settings
ETL Refresh Cycle	1 day/once (can be encrypted and refreshed at key nodes)
Rolling Window Length	7 days
Deviation Trigger Threshold	Key tasks lag > 1 day or > 5%
Cluster Number	3
Time Decay Coefficient	0.05 (recommended range 0.03–0.10)
Closed-loop Overdue Upgrade	Automatically upgrade after 24 hours of overdue

From Table 1, it can be seen that the system has formed a "daily data update + weekly plan rolling + deviation immediate trigger + problem time-limited closed-loop" operation rhythm at the parameter level: ETL ensures the timeliness of the model and on-site data, the rolling window converts the weekly rhythm of construction organization into a calculable unit, the deviation trigger threshold turns "delay" into an identifiable event, the cluster number and time decay coefficient provide adjustable space for quality diagnosis and experience utilization, and the overdue upgrade ensures the rigidity constraint of the work order closed-loop.

At the overall performance level, six 0–1 normalized key indicators (data integrity, collision reduction, progress fulfillment, rework reduction, safety control, and delivery readiness) are selected to compare the two modes, the indicator values are shown in Table 2, and the comprehensive form is shown in Figure 4.

Table 2: Core KPI Comparison (Baseline and CIM-driven).

Indicators	Baseline	CIM-driven	Improvement percentage
Data integrity	0.62	0.88	+0.26
Collision reduction	0.55	0.82	+0.27
Progress fulfillment	0.70	0.86	+0.16
Re-work reduction	0.60	0.80	+0.20
Security control	0.72	0.85	+0.13
Delivery ready	0.58	0.84	+0.26

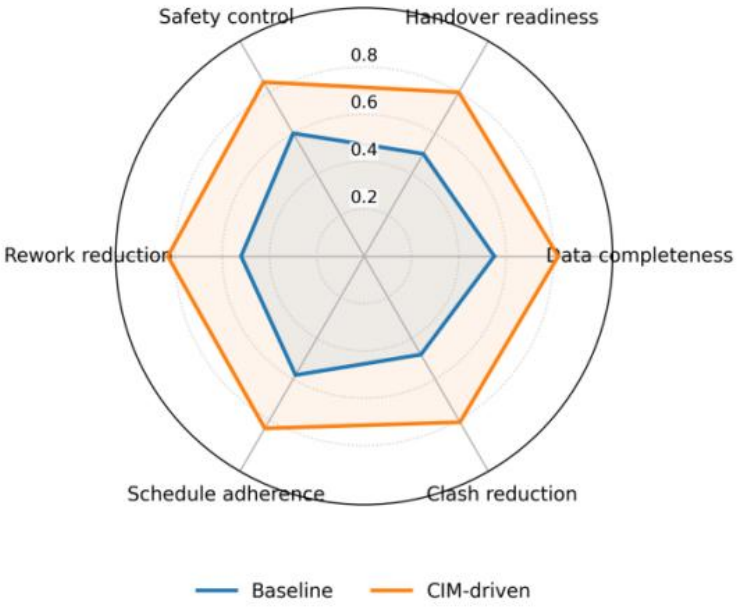

Figure 4: Comparison of KPI Radar between CIM-driven Mode and Baseline Scheme.

From Table 2 and Figure 4, it can be seen that in the CIM-driven mode, all six KPIs are significantly better than the Baseline: Data integrity has increased from 0.62 to 0.88, collision reduction has increased from 0.55 to 0.82, progress fulfillment has increased from 0.70 to 0.86, rework reduction has increased from 0.60 to 0.80, safety control has increased from 0.72 to 0.85, and delivery readiness has increased from 0.58 to 0.84. In the radar chart, the CIM curve expands overall and approaches a regular polygon, while the Baseline curve has a significant "indentation", indicating that the intelligent construction model driven by the urban information model does not only improve in a single indicator, but forms a balanced comprehensive advantage in multiple dimensions such as data, progress, quality, safety, and delivery.

In terms of progress control, a deviation scatter plot is generated based on the planned - actual deviation within a 30-day window, as shown in Figure 5.

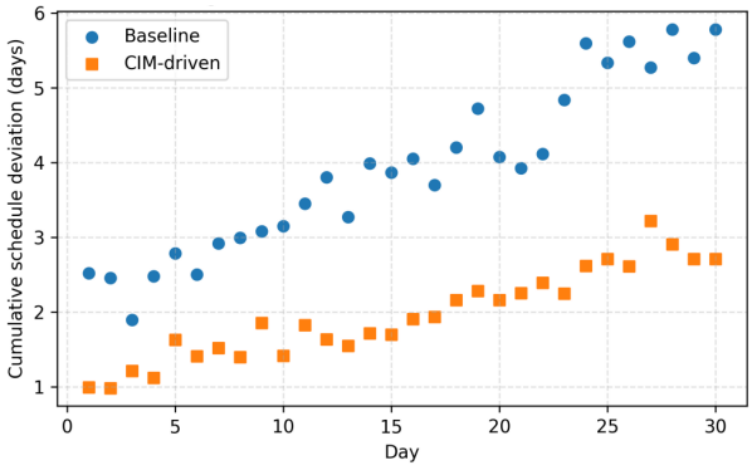

Figure 5: Construction Schedule Plan - Actual Progress Deviation Scatter Plot.

As can be seen from Figure 5, the baseline sample points show a rapid accumulation of deviations in the middle and later stages, with a large degree of dispersion. This indicates that relying on weekly meetings and manual coordination is difficult to timely handle sudden

blockages and resource conflicts; the CIM-driven sample points have a significantly lower and more concentrated overall deviation level, indicating that when the critical tasks lag beyond the threshold, the system can immediately extract the involved tasks and components from the object status records, perform local rearrangement of the critical path and high-conflict tasks using the rolling scheduling algorithm, reallocate time windows and resources, and synchronously write them back to the CIM model and on-site briefing list, thereby controlling the deviation within a smaller range and avoiding large-scale transmission to subsequent processes.

The change of the comprehensive performance score over the weeks is shown in Figure 6.

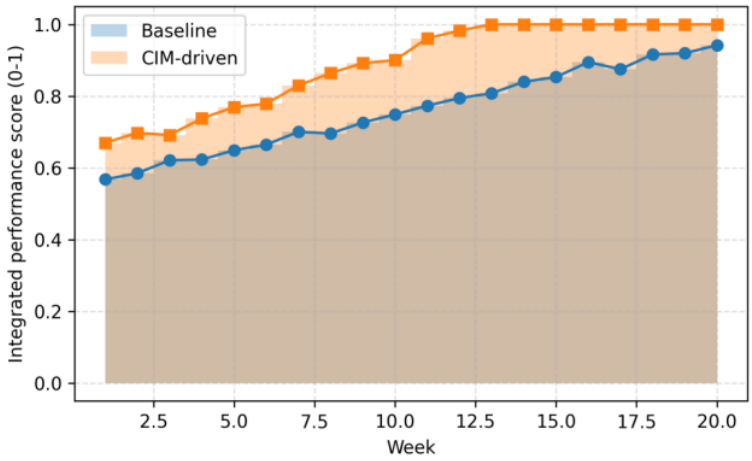

Figure 6: Evolution of Comprehensive Performance Score over Weeks - Area Chart.

In Figure 6, the Baseline area band gradually climbed in the initial weeks and reached a plateau relatively early, indicating that in the traditional model, management improvements mainly relied on phased "concentrated governance" and accumulation of experience; the CIM-driven area band was significantly higher than the Baseline from the initial stage and remained relatively thick around the 8th week, suggesting that the data accumulated from object status recording and closed-loop work orders were continuously used to correct rolling scheduling and inspection strategies, and the system has certain "self-learning" and continuous optimization capabilities. The convergence behavior of risk and defect composite losses corresponding to the comprehensive performance is shown in Figure 7.

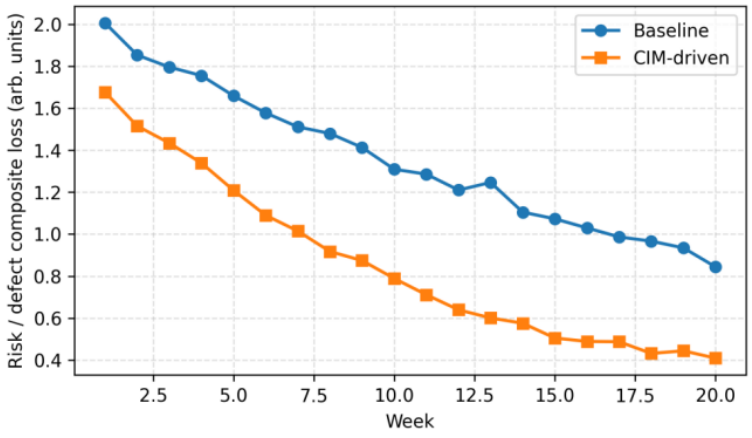

Figure 7: Convergence Curve of Risk/Defect Composite Loss over Weeks.

As shown in Figure 7, the Baseline curve declines slowly with significant fluctuations, especially during the periods of node acceptance and concentrated emergencies, when peaks are prone to occur. This indicates that in the absence of a unified closed-loop mechanism and time-limited handling constraints, problems tend to accumulate and explode in specific stages. The CIM-driven curve declines at a faster rate and has smaller fluctuations, reflecting that the five-state work orders and overdue escalation rules enable problems to complete the closed-loop process of "discovery - assignment - rectification - re-inspection - closure" within a shorter period. The rectification and re-inspection records are promptly filled back into the model and problem database, and unfinished problems are difficult to remain for a long time. The overall risk level shows a stable convergence trend.

The distribution of quality space is presented using a "segmented - defect type heat map", as shown in Figure 8.

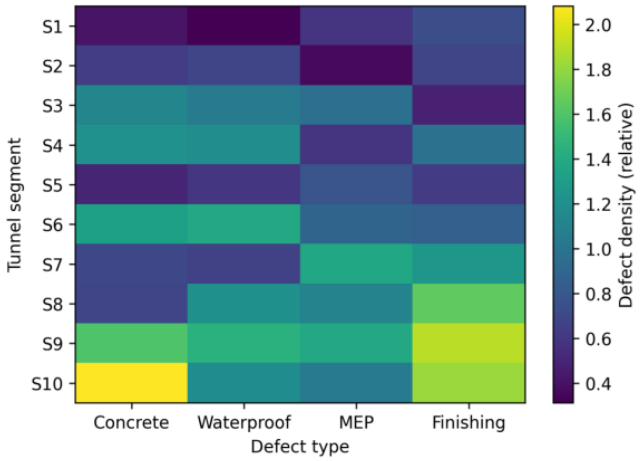

Figure 8: Heatmap of Segmentation - Distribution of Defect Types.

Figure 8 shows that in the CIM-driven mode, during the defect entry stage, it is required to bind object IDs and segments. After clustering based on features such as "segment, defect type, process, and severity", high-frequency defects are represented as continuous "tropical" areas in the heat map. For example, honeycombed rough surfaces of certain structural segments and waterproof leakage in certain compartments show stable high-frequency areas. The system automatically writes these high-frequency clusters into the key inspection points list of the next rolling window and generates corresponding rectification templates and acceptance points, thereby achieving the transformation of high-risk segments and processes from "post-event statistical problems" to "pre-event precise prevention and control".

To assess the extent to which historical records influence current decisions, a sensitivity analysis of the time decay coefficient was conducted, and the results are presented in Table 3.

Table 3: Sensitivity Results of Time Decay Coefficient.

Coefficient	Plan stability (0–1)	Abnormal work order inspection omission rate (%)	Disposal Fairness Index (0–1)
0.01	0.86	7.2	0.92
0.03	0.89	6.1	0.90
0.05	0.91	5.4	0.89
0.10	0.88	6.8	0.79
0.15	0.85	8.5	0.71
0.20	0.83	10.1	0.61

As shown in Table 3, when the time attenuation coefficient is 0.01, the plan stability is 0.86, the missed detection rate is 7.2%, and the fairness index is 0.92. The system gives higher weight to early problems and is prone to focus on the historical high-incidence sections and teams for a long time. When the coefficient increases to 0.05, the plan stability rises to 0.91, the missed detection rate drops to 5.4%, and the fairness remains at 0.89. It takes into account the utilization of historical experience and the identification of new problems. If the coefficient continues to increase to 0.15 or 0.20, the plan stability drops to 0.85 and 0.83 respectively, the missed detection rate rises to 8.5% and 10.1% respectively, and the fairness drops to 0.71 and 0.61 respectively. This indicates that if historical information decays too quickly, the system is more likely to be "driven by recent sporadic events", and the decision-making fluctuations increase. Comprehensive comparison shows that 0.05 is a relatively suitable engineering value.

In terms of noise robustness, by injecting varying degrees of composite noise such as record missing, object connection errors, and duplicate registration into the original records, and comparing the problem identification performance of the Baseline method with the CIM clustering scheme, the results are shown in Table 4.

Table 4: Comparison Results of Problem Identification Robustness under Noise Conditions.

Noise level	Method	Accuracy of problem identification (%)	Cluster consistency (Silhouette)	Dominant cluster distance
10%	Baseline	92.6	—	—
10%	CIM(K-means)	95.1	0.72	0.15
20%	Baseline	88.4	—	—
20%	CIM(K-means)	93.0	0.68	0.18
30%	Baseline	81.7	—	—
30%	CIM(K-means)	89.6	0.61	0.23
40%	Baseline	74.3	—	—
40%	CIM(K-means)	84.9	0.55	0.29

Table 4 shows that as the noise level increased from 10% to 40%, the problem identification accuracy of the Baseline method decreased from 92.6% to 74.3%, while the CIM clustering scheme dropped from 95.1% to 84.9%, with a significantly smaller decline; at the same time, the clustering consistency of the CIM scheme decreased from 0.72 to 0.55, and the dominant cluster internal distance increased from 0.15 to 0.29. Although there was a decline, it still maintained a relatively clear cluster structure, indicating that through the strategy of "dominant cluster-driven key inspection and outlier cluster diversion and re-examination", the risk identification ability remained relatively stable under the condition of poor record quality.

3.2 Evaluation of the Application Effect of the Underground Pipeline Tunnel Smart Operation and Maintenance Management Mode Driven by the Urban Information Model

During the operation and maintenance phase, the urban information model is used as the unified asset and spatial data foundation. The monitoring data flow, inspection records, alarms and work orders, etc. are linked at multiple hierarchical objects such as "structures - compartments - equipment - sensors". Two modes, namely the traditional operation and maintenance group

(Traditional O&M, relying on manual inspection + scattered SCADA screens + Excel ledgers) and the CIM-driven operation and maintenance group (CIM-driven O&M, adopting CIM + online monitoring + alarm work order platform), are set up within the same underground pipe corridor section for comparative evaluation. The corresponding relationships between operation scenarios, key data sources, calculation rules and output indicators are shown in Table 5. Daily inspections and defect records are matched with objects through the inspection APP and CIM component codes. Environmental and safety monitoring identifies over-limit risks based on threshold and trend anomaly detection. Equipment status assessment and pre-maintenance generate pre-maintenance lists through health score and fault probability estimation algorithms. Energy consumption monitoring and energy-saving diagnosis rely on baseline benchmarking and itemized energy consumption attribution to locate high-energy consumption segments. Alarm and work order closed-loop management achieves full-process traceability through alarm classification, automatic assignment, overdue escalation and closed-loop statistics.

Table 5: Comparison of Operation and Maintenance Scenarios with CIM-Driven Function Modules.

O&M scenario	Key data sources	Main algorithms / rules	Core outputs	O&M scenario
Routine inspection & defect logging	Inspection app records, CIM component codes, photos / videos	Object matching, inspection compliance rules	Inspection completion rate, defect list	Routine inspection & defect logging
Environmental & safety monitoring	Sensor data for water level, temperature and humidity, gas concentration, smoke detection, etc.	Threshold-based and trend anomaly detection, sliding-window smoothing	Over-limit alarms, risk levels	Environmental & safety monitoring
Equipment condition assessment & pre-maintenance	Operating current, voltage, start–stop counts, historical fault records	Health scoring, remaining-life estimation, failure probability estimation	Equipment health scores, preventive maintenance suggestions	Equipment condition assessment & pre-maintenance
Energy monitoring & energy-saving diagnostics	Power / water metering data, equipment running hours	Baseline benchmarking, sub-item energy attribution, load-curve decomposition	Sub-item energy consumption, identified energy-saving potential	Energy monitoring & energy-saving diagnostics
Alarm & work-order closed-loop management	Alarm logs, work-order workflow records, CIM spatial locations	Alarm grading, automatic dispatching, overdue escalation, closed-loop statistics	Response time, closure time, overdue rate	Alarm & work-order closed-loop management

In terms of overall operational performance, six 0–1 normalized indicators - inspection coverage rate, fault detection rate, average repair time score, energy consumption performance,

data integrity, and remote control capability - were selected as the operational KPIs. The comparison results are shown in Table 6 and Figure 9. Under the CIM-driven mode, all six indicators were significantly higher than those in the traditional mode. Specifically, the inspection coverage rate increased from 0.68 to 0.90, the fault detection rate from 0.70 to 0.92, the average repair time score from 0.60 to 0.82, the energy consumption performance from 0.65 to 0.88, data integrity from 0.62 to 0.90, and remote control capability from 0.55 to 0.86. This demonstrates the collaborative optimization effect of inspection route planning, anomaly identification, maintenance scheduling, and energy consumption management under the unified CIM base.

Table 6: Comparison of Operational KPIs (Traditional O&M vs. CIM-driven O&M).

Indicator	Traditional O&M	CIM-driven O&M
Inspection coverage	0.68	0.90
Fault detection rate	0.70	0.92
Average repair time score	0.60	0.82
Energy performance	0.65	0.88
Data completeness	0.62	0.90
Remote control capability	0.55	0.86

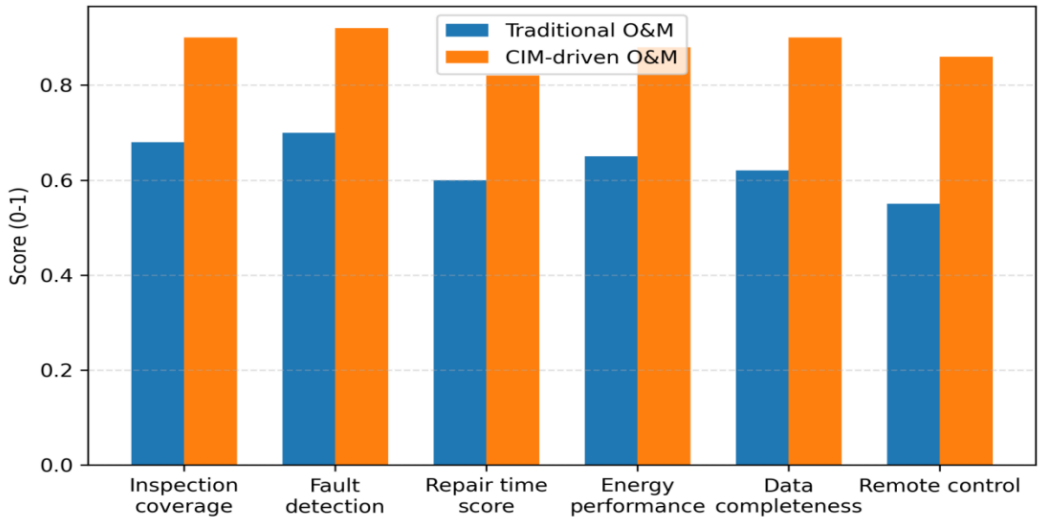

Figure 9: Comparison of Key Performance Indicators for Underground Pipeline Maintenance Operations.

In terms of alarm handling, the number of trigger times, average response time, and closed-loop time for different levels of alarms within the same period were statistically analyzed. The results are shown in Figure 10 and Table 7. It can be seen that under the CIM-driven mode, the average response times for Level I major alarms, Level II general alarms, and Level III warning alarms were reduced from 31.5 minutes, 42.7 minutes, and 55.3 minutes to 14.2 minutes, 20.6 minutes, and 28.4 minutes respectively, and the corresponding closed-loop times were shortened from 6.8 hours, 12.5 hours, and 24.7 hours to 3.1 hours, 6.9 hours, and 11.2 hours. This is due to the alarm classification and automatic dispatching algorithm based on the spatial position and equipment level of CIM - the system automatically matches the responsible position and duty personnel according to the alarm level and impact range, pushes the alarm through the mobile terminal and guides the shortest path to the site. If the time limit is exceeded, it automatically upgrades to the superior duty personnel, forming quantifiable improvement in

handling efficiency.

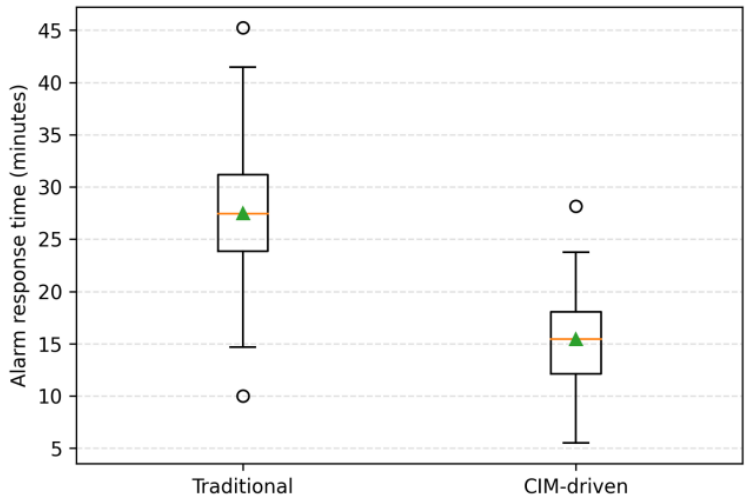

Figure 10: Box plot of alarm response time distribution.

In order to avoid the subjective perception bias caused by the graphical presentation and to facilitate the subsequent horizontal comparison of different projects and different operation and maintenance stages, this paper further lists the normalized scores of each indicator in the figure in numerical form in Table 7, and quantitatively depicts the differences in key performance indicators between the two operation and maintenance modes with greater accuracy.

Table 7: Statistical Comparison of Equipment Health and Failure Rate.

Indicators	Traditional O&M	CIM-driven O&M
Average equipment health index	0.67	0.88
Annual failure rate (times per unit per year)	0.42	0.21
Proportion of sudden outage incidents (%)	37.5	18.3

In terms of energy consumption performance, based on the monthly energy consumption data of the pipe gallery power distribution and environmental control systems over a 12-month period within a typical operation cycle, a violin plot was used to depict the energy consumption distribution characteristics, as shown in Figure 11. The violin plot indicates that the overall range of monthly energy consumption distribution in the traditional mode is relatively high, with a wide distribution width. However, in the CIM-driven mode, the energy consumption moves downward overall and is more concentrated in distribution. In terms of the implementation path, the system attaches the branch metering data to the CIM objects, decomposes the energy consumption by cabin and equipment type, and the operation and maintenance algorithm compares the energy consumption per unit length of the pipe gallery and per unit equipment under different operating conditions, identifies the segments with high energy consumption, and combines with time series analysis to propose strategies such as reducing the speed of the fan at night, controlling the lighting in a hierarchical manner, and fine-tuning the set temperature of the air conditioning, thereby bringing about changes in the overall energy consumption distribution.

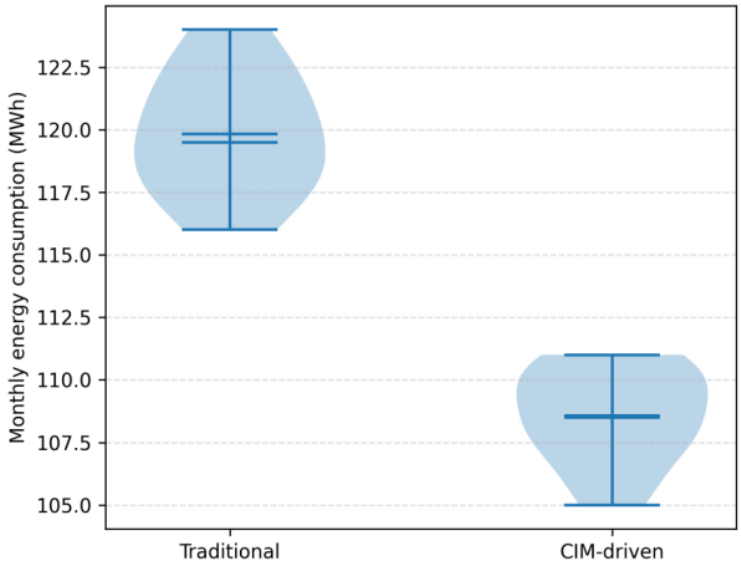

Figure 11: Monthly Energy Consumption Distribution of Underground Pipeline Structure (Violin Plot).

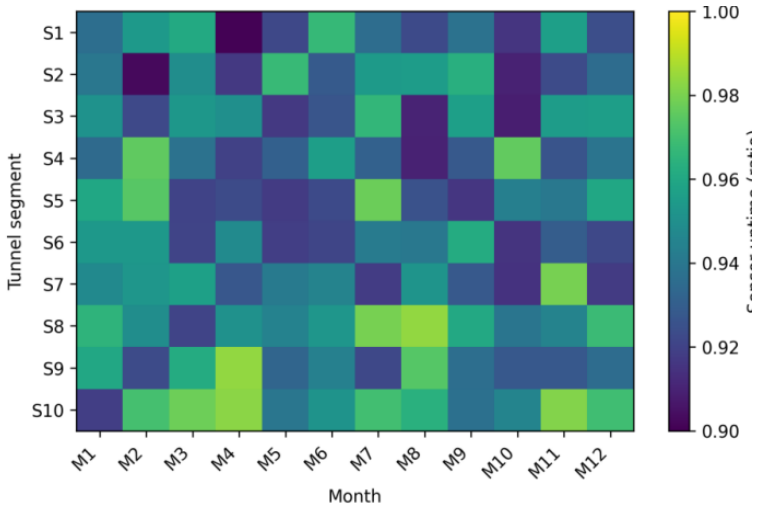

Figure 12: Heatmap of Sensor Online Rate.

By integrating the results from Tables 1 to 7 and Figures 4 to 12, it can be observed that the intelligent operation and maintenance management model driven by the urban information model for underground pipe galleries has achieved quantifiable improvements in multiple aspects such as inspection coverage, fault detection, repair timeliness, energy consumption performance, data integrity, and monitoring network reliability. These improvements directly stem from the data integration and algorithm application "centered on CIM" in the operation and maintenance process: On one hand, through object-oriented data modeling, anomaly detection, health assessment, pre-maintenance recommendations, and energy consumption diagnosis algorithms, the forward-looking nature of problem discovery and resolution has been significantly enhanced; on the other hand, through alarm classification and work order closed-loop mechanisms, the operation and maintenance behaviors can be tracked and optimized both in time and space, providing a reusable model for the promotion in the operation and maintenance management of larger-scale urban underground spaces in the future.

4 Discussion

The current research on underground integrated pipe galleries mainly focuses on single engineering or single professional issues such as structural stress and geological disaster response, ventilation and energy conservation, as well as construction environment management. Typical works have provided important conclusions from aspects such as flexible joints, ground fissure effects, shallow-buried deformation, ventilation pre-cooling and environmental management systems. However, the data organization is still mainly centered around isolated projects and local conditions, and has not yet formed a unified information base at the urban scale. Meanwhile, research on CIM/GIS and intelligent algorithms for urban buildings, transportation, and green spaces has demonstrated strong potential in directions such as fire evolution simulation, smart city governance, urban energy-microclimate coupling, open space mapping, and traffic state prediction. However, the underground pipe galleries, a typical "urban lifeline", have not yet been incorporated into a unified urban information model system. Based on this, this paper constructs a multi-source data integration and optimization decision-making framework that runs through surveying, design, construction, and operation and maintenance, using a three-layer CIM data model at the urban, project, and asset levels. It integrates collision control, 4D construction rolling scheduling, defect clustering, equipment health assessment, and energy consumption diagnosis algorithms onto the objectified CIM base, achieving an extension from "single-point experiments, single-line monitoring" to "urban-level integrated management". The engineering application results show that the data integrity during the construction phase has increased from 0.62 to 0.88, the collision reduction index has increased from 0.55 to 0.82, and the progress performance has increased from 0.70 to 0.86. During the operation and maintenance phase, the inspection coverage rate and fault detection rate have increased from 0.68 and 0.70 to 0.90 and 0.92, with the annual failure rate decreasing from 0.42 to 0.21 failures per unit per year. The proportion of sudden outages has decreased from 37.5% to 18.3%, and the online rate of sensors has remained above 0.94 for a long time. This indicates that the data integration based on CIM and the "monitoring–prediction–work order" closed-loop algorithm can effectively transform the advantages of urban-level spatial information into quantitative performance improvements in the construction and operation of underground pipe galleries. It should be noted that this research is still limited by a single-city sample and limited pilot sections. Some parameters, such as time attenuation coefficients and deviation trigger thresholds, have scene-related characteristics, and the algorithm forms are mainly based on interpretable rules and optimization. The potential for mining spatio-temporal correlations using deep learning and graph models is insufficient, and the coupling with urban-level energy consumption, microclimate, and traffic models is still in the initial stage. This leaves room for further deepening and cross-integration in subsequent promotion and expansion of "CIM-driven intelligent construction and management of underground pipe galleries" under multi-city and multi-system conditions.

5 Conclusion

This research is based on a three-tier CIM data model at the city-level, engineering-level and asset-level, and has constructed an integrated management and construction model for underground integrated pipe galleries, featuring "multi-source data integration - collaborative design and construction rolling scheduling - intelligent operation and maintenance loop". Engineering application results show that the data integrity during the construction phase has increased from 0.62 to 0.88, the collision reduction index has risen from 0.55 to 0.82, the progress fulfillment has improved from 0.70 to 0.86, and the KPIs such as reduction of rework,

safety control and readiness for delivery have all increased by 0.13 to 0.27. When the time attenuation coefficient is set at 0.05, the plan stability reaches 0.91, and the abnormal work order missed detection rate drops to 5.4%. This proves that the collaborative design optimization based on CIM constraints and 4D rolling scheduling can significantly enhance the planning execution and quality control capabilities of pipe gallery construction. In the operation and maintenance stage, the inspection coverage rate and fault detection rate have increased from 0.68 and 0.70 to 0.90 and 0.92, the average repair time score has improved from 0.60 to 0.82, the annual failure rate has decreased from 0.42 to 0.21 times per unit per year, the proportion of sudden outages has dropped from 37.5% to 18.3%, the online rate of typical segment sensors has remained above 0.94 for a long time, and the monthly energy consumption distribution has shifted downward and the dispersion has decreased. This indicates that the "monitoring - prediction - work order" chain and health assessment, energy consumption diagnosis algorithms can effectively support the transformation of underground pipe galleries from passive repair to active prevention and precise energy conservation, providing a replicable technical path for the high-quality construction and resilient operation and maintenance of underground infrastructure in the context of smart city renewal.

Funding

1. Project of the Sichuan Technology and Business University: Research on Safety Intelligent Monitoring and Operation and Maintenance Optimization of Underground Utility Tunnels in Existing Residential Areas for Urban Renewal Based on CIM(XJ2025YB020)

2. Project of the China Adult Education Association: Research on the Path and Cases of Art Education Empowering Rural Revitalization and Regional Development - Taking Chengdu as an Example (YS-YB2025001S)

About the Author

Xuehao Chen, an associate professor, was born in Zhangye, Gansu, P.R. China,in 1986.He obtained his master's degree from Southwest Jiaotong University in China. Recently,he teaches at Sichuan Technology and Business University. His main research direction is the integrated application of City Information Modeling (CIM).
ce.chenxuehao@foxmail.com

Ruiming Lan, was born in Chengdu, Sichuan,P.R. China,in 1998.He obtained a master's degree from Chongqing Technology and Business University in China. Recently, hehave been teaching at the School of Business of Southwest Jiaotong University Hope College. His main research direction is urban economy and management.
cimstudio@163.com

References

[1] Enhua Zhang, Haiying Cao, Ping Wang, Zhen Zhao & Jiefeng Liu. (2025). Investigation on the Mechanical Response of a Prefabricated Underground Pipe Gallery with a Flexible Energy Dissipation Node: An Experimental Study. Buildings, 15(19), 3521-3521. https://doi.org/10.3390/BUILDINGS15193521.

[2] Tong Wei, Haonan Jiang, Chengqian Xu, Zhaolin Gu, Bin Yang & Xilian Luo.(2025). Optimizing built-in chimney ventilation: Synergetic effects of underground pipe gallery

pre-cooling and PV/T post-heating. Renewable Energy, 255, 123770-123770. https://doi.org/10.1016/J.RENENE.2025.123770.

[3] Soukaina Bakkass,Naoual Semlali aouragh Hassani,Mohammed Karim Ben hachmi & Abderrahim El Hilali.(2025).Implementation of an environmental management system (ISO 14001) on an underground gallery construction site in Casablanca Morocco.Cleaner Waste Systems,11,100259-100259.https://doi.org/10.1016/J.CLWAS.2025.100259.

[4] Haoyue Lin,Zehua Yin,Chunwu Wang,Yifan Lin,Muhammad Suhail Shaikh,Chang Wang & Xiaoqing Dong.(2025).Efficient Positioning Method for Underground Pipe Gallery Inspection Based on UWB Adaptive Fusion.IET Communications, 19(1), e70037-e70037.https://doi.org/10.1049/CMU2.70037.

[5] Xintao Yu,Baoan Han,Yubo Zhao,Botuan Deng,Kang Du & Haosheng Liu.(2025).A Study on the Calculations of the Bottom Void Range of an Underground Pipe Gallery Structure Under the Action of Ground Fissure Dislocations. Buildings, 15(6), 920-920. https://doi.org/10.3390/BUILDINGS15060920.

[6] Tong Wei, Cong Shen, Haonan Jiang, Zijun Xu, Zhaolin Gu & Xilian Luo.(2025). Experimental study on cooling performance of underground pipe gallery ventilation enhanced by borehole heat exchanger.Renewable Energy, 240, 122134-122134. https://doi.org/10.1016/J.RENENE.2024.122134.

[7] Moussa Diallo, Ahmed Amara Konaté & Diaka Sidibé.(2024).Collapse of underground galleries in gold-panning mines: Perception of stakeholders in the Doko Sub-Prefecture, Siguiri Prefecture, Republic of Guinea. Environmental & Socio-economic Studies, 12(3),23-36.https://doi.org/10.2478/ENVIRON-2024-0017.

[8] Gaifang Xin, Jun Zhu & Jing Tang.(2024). WSNs distributed sensing of mobile robot under the irregular topology of underground pipe gallery.International Journal of Computational Science and Engineering, 27(2), 230-237. https://doi.org/10.1504/IJCSE.2024.137293.

[9] Dorthi Kumar & Karra Ram Chandar.(2022).Integrated Slope Monitoring System for Slope Stability Over Old Underground Galleries During Surface Mining Operations Using Internet of Things. Geotechnical and Geological Engineering, 41(3), 1763-1775. https://doi.org/10.1007/S10706-022-02369-2.

[10] Deng Bo tuan,Li Pan,Li Xin,Tian Jiang tao & Zhi Bin.(2022).Mechanical behavior of underground pipe gallery structure considering ground fissure.Journal of Mountain Science,19(2),547-562.https://doi.org/10.1007/S11629-021-6867-3.

[11] Xie Junfei,Huang Nenghao,Feng Jiajia & Zhang Gen.(2020).Study on Deformation of Shallow Buried Underground Pipe Gallery.IOP Conference Series: Materials Science and Engineering,741,012058-012058.https://doi.org/10.1088/1757-899x/741/1/012058.

[12] Bin Sun.(2025).Theoretical model and prediction framework for rapid fire evolution simulation of urban buildings based on geographic information system.Sustainable Energy Technologies and Assessments, 84, 104710-104710. https://doi.org/10.1016/J.SETA.2025.104710.

[13] Luqi Wang,Jinrui Li,Wenyi Cen & Weimin Feng.(2025).Governing sustainable smart cities supported by city information modelling: a bibliometric analysis and systematic review.Journal of Asian Architecture and Building Engineering, 24(5), 4433-4451. https://doi.org/10.1080/13467581.2024.2399680.

[14] Sungyeol Lee,Jaemo Kang,Jinyoung Kim & Myeongsik Kong.(2025).AI-Based Damage Risk Prediction Model Development Using Urban Heat Transport Pipeline Attribute Information.Applied Sciences,15(14),8003-8003.https://doi.org/10.3390/APP15148003.

[15] Yulia Karpova, Fulgencia Villa, Eva Vallada & Wanzhen Ana Pan.(2025).A Multi-Objective Model in Combination with Geographic Information System Tools for the Location of Urban Green Areas. Mathematics, 13(12), 2006-2006. https://doi.org/10.3390/MATH13122006.

[16] Maosu Li, Fan Xue & Anthony G.O. Yeh. (2025). Efficient and accurate assessment of window view distance using City Information Models and 3D Computer Vision. Landscape and Urban Planning, 260, 105389-105389. https://doi.org/10.1016/J.LANDURBPLAN.2025.105389.

[17] Na Luo,Xuan Luo,Mohammad Mortezazadeh,Maher Albettar,Wanni Zhang,Dongxue Zhan... & Tianzhen Hong.(2025).A data schema for exchanging information between urban building energy models and urban microclimate models in coupled simulations. Journal of Building Performance Simulation, 18(3), 333-350. https://doi.org/10.1080/19401493.2022.2142295.

[18] Zijian Xu,Jiajun Chen,Hongyang Niu,Runyu Fan,Dingkun Lu & Ruyi Feng. (2025). Boosting Urban Openspace Mapping with the Enhancement Feature Fusion of Object Geometry Prior Information from Vision Foundation Model.Remote Sensing, 17(7), 1230-1230.https://doi.org/10.3390/RS17071230.

[19] Anran Li,Zhenlin Xu,Wenhao Li,Yanyan Chen & Yuyan Pan.(2025).Urban Signalized Intersection Traffic State Prediction: A Spatial–Temporal Graph Model Integrating the Cell Transmission Model and Transformer.Applied Sciences, 15(5), 2377-2377. https://doi.org/10.3390/APP15052377.

[20] Ahmad Askari Lasaki, Mohammad Reza Adlparvar & Mahtiam Shahbazi.(2024).An integrated soft computing-based criteria interdependencies and intuitionistic fuzzy information to evaluate the urban concrete bridge maintenance models.Soft Computing, 28(13-14), 8105-8117.https://doi.org/10.1007/S00500-024-09678-Z.